

Structural Analysis of Aerodynamic Brakes in High-Speed Trains

Ivana Vasović¹⁾
Mirko Maksimović²⁾
Mirjana Puharić¹⁾
Dušan Matić¹⁾
Suzana Linić¹⁾

Aerodynamic problems in railway trains are closely associated with flows occurring around trains. The main objective of this paper is to present the results of the finite element method for stress and stability analysis of aerodynamic brakes in high speed trains (HST). The aerodynamic brake is defined as a stiffened plate subjected to lateral pressure load considering buckling behaviour. The shell finite elements are used to model a stiffened type construction. A well-established commercially available Finite Element program MSC/NASTRAN has been chosen for the purpose. The CFD analysis is used to determine aerodynamic load.

Key words: train, aerodynamic brake, aerodynamic load, stress state, stress analysis, stability analysis, fluid dynamics, numerical simulation, finite element method.

Introduction

IN general, aerodynamic brakes have been used in the domain of aircraft and flight constructions as well as for high-speed trains. The attention in this work is focused on the minimum weight design of aerodynamic brakes in high-speed trains (HST). The finite element method [3] is used for the stress/strength analysis of brakes. For a precise aerodynamic load distribution, the Computation Fluid Dynamic (CFD) method [4] is used.

Aerodynamic problems linked with high-speed train systems are nowadays receiving a considerable attention as practical engineering problems. With train speed increase, many engineering problems, which have been reasonably neglected at low speeds, are being raised with regard to aerodynamic noise and vibrations, impulse forces occurring as two trains intersect each other, impulse wave at the exit of tunnel, ear discomfort of passengers inside the train, etc. These are some of major limiting factors to the increase of train system speed. Such aerodynamic problems are closely associated with the flows occurring around railway trains.

Besides conventional brakes, high-speed trains also use aerodynamic brakes as additional braking systems. Aerodynamic brakes are designed to generate a braking force by increasing a drag by pulling the panels on the car roof, thus increasing the surface area exposed to the incoming air stream.

When the aerodynamic brake is in the extended position, it blocks the airflow and overpressure occurs in front of it, while behind it an area of negative pressure is formed due to the flow separation behind the plate. The difference in pressures between the front and the rear brake panel surface creates a resistance force normal to the surface of the panel and serves as a braking force. The tangential force induced

by the surface friction is negligible when compared to the normal force.

An aerodynamic train drag increases with the square of speed, and an aerodynamic brake system has a very good performance, particularly at high speeds. Therefore, aerodynamic brakes are classified as high speed brakes. It is very interesting to determine their effectiveness when a train reaches speeds higher than 100 m/s. An aerodynamic brake is considered as a stiffened aluminium plate. Stiffened plates are basic building elements in many civil as well as aircraft structural applications and, as such, accurate strength assessment of individual stiffened plate components is one of the key parameters to perform a general strength analysis. These structural components typically consist of a plate with equally spaced stiffeners (flat bar or T- and L- sections welded on one side) and often with intermediate transverse stiffeners, frames or bulkheads.

Stiffened plates in high-strength aluminium alloys have been used in a variety of marine structures, with applications such as hull and decks in high-speed boats and catamarans and super- structures for ships. Other applications are bridge box girders, and walls and floors of offshore modules and containers. These elements are primarily required to resist axial compressive forces (induced by hull bending moment) as well as lateral loads arising from different sources like hydrostatic/hydrodynamic pressures or cargo weight.

The literature on stiffened aluminium panels is more limited. Clarke and Narayanan [3] report on buckling tests on an aluminium AA5083 plate with welded T-bar and flat bar stiffeners. His experimental programme comprised eight compression tests on panels with different plate and stiffener sizes with buckling over two spans as the failure mode.

¹⁾ Institute GOŠA d.o.o., Milana Rakića 35, 11000 Belgrade, SERBIA

²⁾ Belgrade Waterworks and Sewerage, Kneza Miloša 27, 11000 Belgrade, SERBIA

The ultimate strength of stiffened aluminium AA6082-T6 plates under axial compression was investigated by Aalberg et al. [6, 7] using numerical and experimental methods.

Khedmati et al. [8] made an extensive sensitivity analysis on buckling and ultimate strength of continuous stiffened aluminium plates under combined in-plane compression and different levels of lateral pressure.

The present work consists of two parts; Part I deals with the aerodynamic load distribution of train brakes, and Part II treats stiffened panels surrounded by strong support members such as longitudinal girders and transverse frames.

In this paper, the buckling behaviour and ultimate strength characteristics of stiffened aluminium plates under lateral pressure load are investigated using the finite element method. The plate dimensions, stiffener types and stiffener dimensions are varied in a systematic manner in the analysis.

Aerodynamic calculation of resistance for flat panels placed perpendicularly to the flow

Roof-mounted brakes have the following dimensions: $b = 1.5$ m and $c = 0.9$ m. From the diagram in Fig.1, for the ratio $b/c = 1.67$, the drag coefficient $C_x = 1.14$ is obtained [1,2].

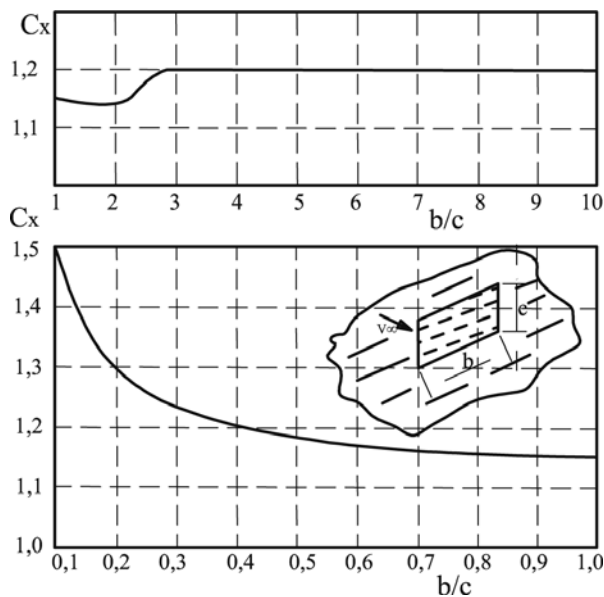


Figure 1. The coefficient of the drag of flat plates placed perpendicularly to the flow

The aerodynamic drag per unit area is calculated from equation [1,2]:

$$\frac{F_x}{A} = C_x \frac{1}{2} \rho V^2 \quad \frac{N}{m^2} \quad (1)$$

The aerodynamic drag per unit area of flat plates is given in Table 1.

Table 1. Aerodynamic drag per unit area of flat plates

Number of panels n	1	2	3
$\Delta F_x/A$ kN/m ²	3.42	2.20	2.14

Train and aerodynamic brake geometry

The simulations are made for a train with two locomotives, at each end, and four passenger cars between them. The length of the locomotives and the wagons is 20 m and the gap between cars is 0.2 m, so that the total length of the composition is $L = 121$ m. Fig.2a gives a view of the train cross section and the brake positions. Fig.2.b gives a position of the first brake, at a distance of 6 m from the nose of the train, while Fig.2c gives the position of the second brake, placed at a distance of 17 m behind the first one. The third brake is placed at a distance of 20 m behind the second one.

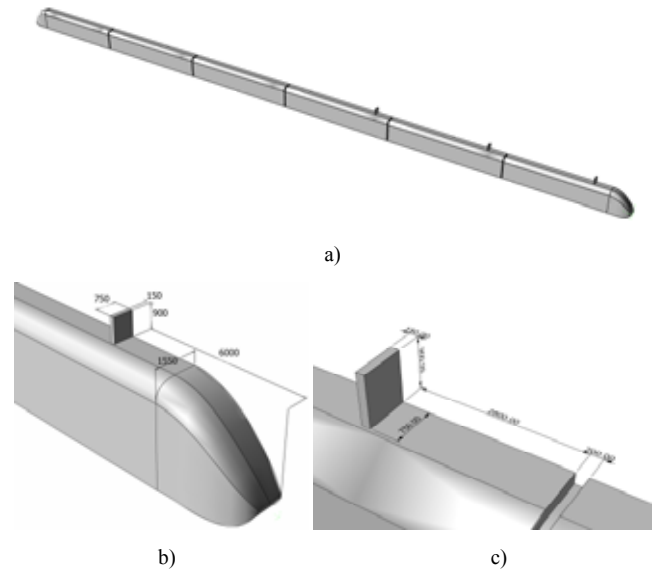


Figure 2. Train cross section and the positions of aerodynamic brakes

- Braking force

Drag forces, in the cases of the train without brakes, with pulled 1, 2 and 3 aerodynamic brakes, obtained by FILUENT simulations, are presented in Table 2.

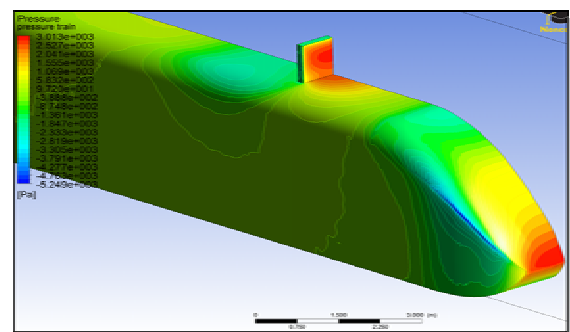


Figure 3. Pressure distribution around the aerodynamic brake

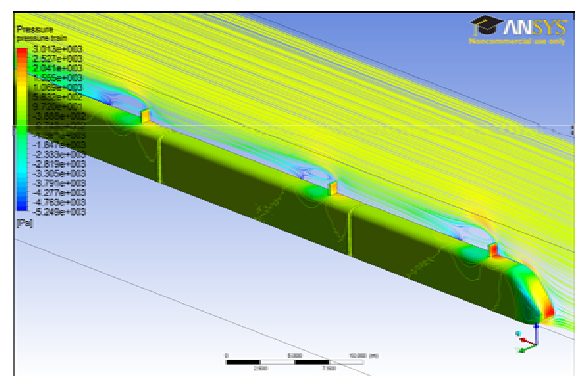


Figure 4. Streamlines around the aerodynamic brakes on the roof of the symmetry plane

Table 2. Drag forces

The number of brakes n	0	1	2	3
Drag force F_x kN	20.61	25.47	28.6	31.64

The contribution to the drag force per unit area of each brake to the overall aerodynamic train drag was calculated as follows:

$$\frac{\Delta F_{xn}}{A_{koc}} = \frac{F_{xn} - F_{x(n-1)}}{A_{koc}} \quad \frac{kN}{m^2} \quad (2)$$

where:

- ΔF_{xn} – contribution of each brake individually to the overall aerodynamic train drag
 F_{xn} – drag force, when the number of open brakes is n
 A_{koc} – panel area of the aerodynamic brakes ($A_{koc}=1.35 \text{ m}^2$).

Table 3 shows the contribution of each brake individually to the overall aerodynamic resistance.

Table 3. Contribution to the train drag force

The number of brakes n	1	2	3
Contribution to the train drag force $\Delta F_{xn}/A_{koc}$ kN/m ²	3.6	2.32	2.25

The comparison of the results obtained using the FLUENT by simulating the flow around the train with aerodynamic brakes and the results obtained by the drag calculation of flat plates placed normally to the direction of air flow provides a good agreement. The results of simulations using the FLUENT are expected and applicable to other train speeds.

From the braking force obtained by simulation using the FLUENT, we can determine the brake drag coefficient as follows:

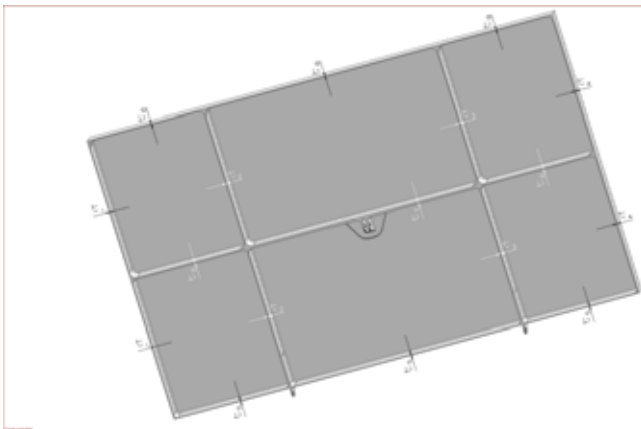
$$C_x = \frac{\Delta F_{xn}}{1/2 \rho v^2 A_{koc}} \quad (3)$$

The drag coefficient for the first brake obtained by the FLUENT simulation is $C_x = 1.199$. The aerodynamic drag force of the brakes for different speeds can be calculated from the expression:

$$F_x = C_x \cdot \frac{1}{2} \rho v^2 \cdot A_{koc}$$

Structural analysis of brakes by finite elements

The subject of this section is the stress and stability analysis of aerodynamic brakes. The aerodynamic brake is designed as a stiffened aluminum plate.

**Figure 5.** Geometric properties of aerodynamic brakes.

In this study, the commercially available finite element code NASTRAN [7] was used for the stress analysis. Both the plate and the stiffeners are modeled using shell finite elements selected from the NASTRAN library of elements. The geometry properties of aerodynamic brakes are shown in Fig.5.

The finite element model of aerodynamic brakes and the boundary conditions are shown in Fig.6.

Table 4. Geometry properties of aerodynamic brakes for various models

Model No.	t [mm]	t_1 [mm]	t_2 [mm]	t_3 [mm]	t_4 [mm]	t_5 [mm]	t_6 [mm]	t_7 [mm]
1	10	10	10	10	10	10	10	10
2	5	3	3	3	3	3	3	10
3	3	2,5	2,5	2,5	2,5	2,5	2,5	10
4	5	3	3	3	3	3	3	8

The finite element model of aerodynamic brakes and the boundary conditions are shown in Fig.6.

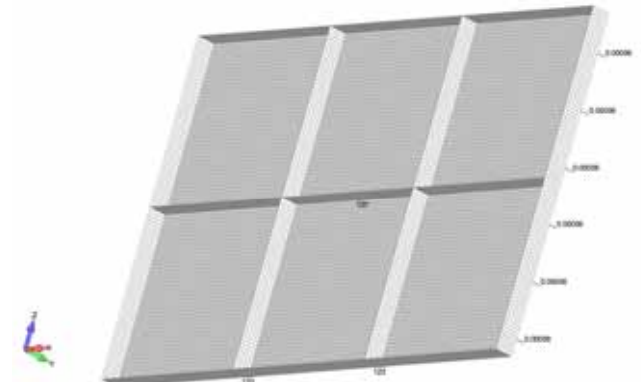
**Figure 6.** Finite element model of the aerodynamic brake

Fig.6 shows the finite element model of aerodynamic brakes prepared in the MSC NASTRAN software package. There is the shell model for the given geometry of the brake and the boundary conditions and loads as shown in Fig.6. The brake material is aluminium plate. In the first case the thickness of the plate and ribs is 10 mm (Model 1, Table 3). Fig.7 shows the stress distribution and the critical zones and deflection.

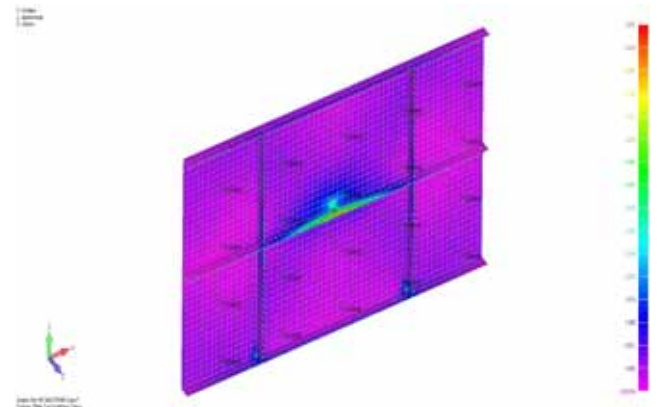
**Figure 7.** Stress distribution in the brake under external pressure (Model 1)

Fig.7 shows the aerodynamic brake under pressure obtained using the CFD analysis in the FLUENT software package¹⁰. The aerodynamic brake is in the stress state (VonMises's stress) obtained using FEM and NASTRAN software package. The finite element method was used to calculate the stress of the panel and the ribs and strakes that are set up as a reinforcement on the panel - brake. The

maximum stress obtained was 7.271 daN/mm^2 , which is completely within the tolerable limits. The maximum displacement on the construction was 3.47 mm , which is also within the permitted limits. The thickness of all elements of the structure was 10 mm . As the stress was much lower than the allowable one, it was considered to reduce the thickness of the elements but not continuously, and the plate was 5 mm thick, strakes and ribs were 3 mm thick each and the central rib was 10 mm thick (Model 2, Table 4). In this case the maximum stress was 12.15 daN/mm^2 and the maximum displacement was 7.1 mm . It can be therefore seen how the stress increased and how the movement increased significantly. In order to reduce the weight of the aerodynamic brakes, the next step was to reduce the thickness as it did not exceed the permissible stress limit. The results are shown in Fig.8.

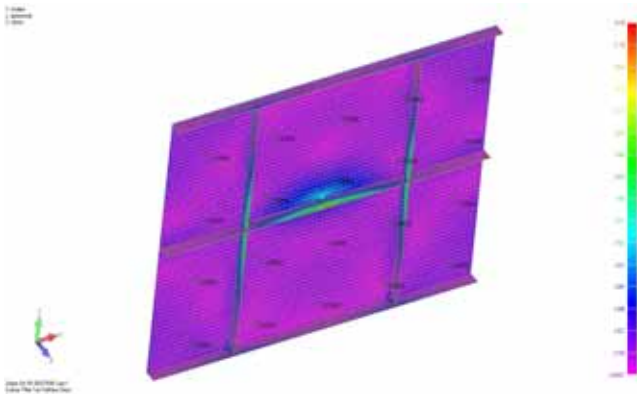


Figure 8. Stress distribution in the brake under external pressure (Model 2)

The maximum stress is 12.15 daN/mm^2 and the displacement is 7.1 mm max. The thickness of the plate is 5 mm , the thickness of the strakes and ribs is 3 mm and the central rib is 10 mm thick.

The following figure shows a prepared model with the thickness further reduced, and the brake weight consequently.

When the plate thickness is 3 mm with the thicknesses of the ribs and strakes of 2.5 mm and the central rib is left to be 10 mm (Model 3, Table 4), the stress is 13.22 daN/mm^2 and the displacement is 8.62 mm , Fig.10.

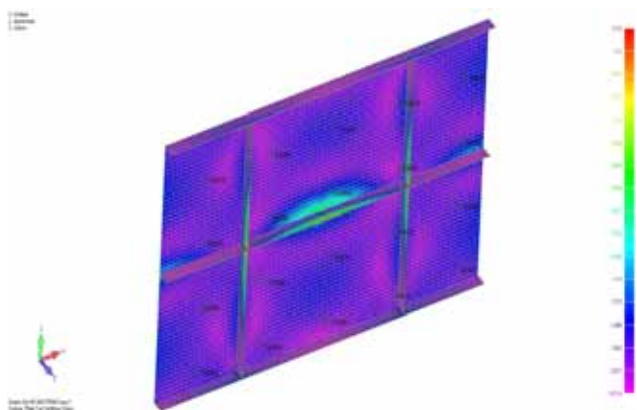


Figure 9. Stress distribution in the brake under external pressure (Model 3)

Fig.9 presents the results of the stress state in the aerodynamic brake with the practically minimum dimensions of ribs, strakes and the plate. The minimum sizes are used in terms of production technology using the technology of brake milling.

To obtain the minimum weight of the construction, the dimensions are reduced to satisfy allowable stresses of

aluminium material properties and buckling load behaviour (Model 4, Table 4). The complete results are shown in Figs. 10 to 12.

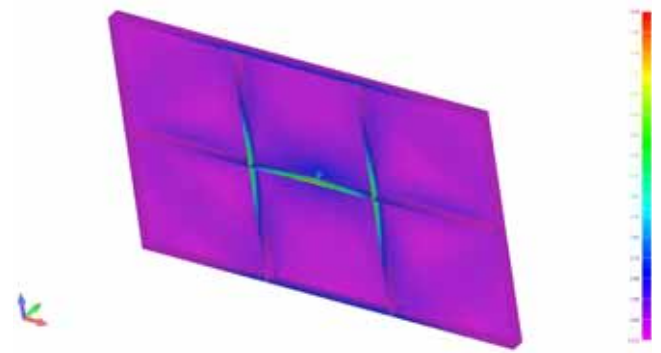


Figure 10. Stress distribution in the brake under external pressure (Model 4)

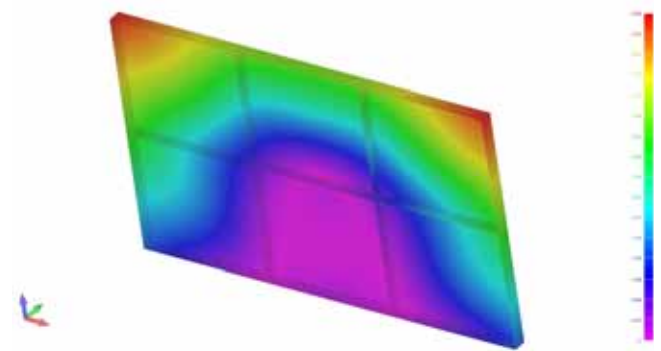


Figure 11. Displacement distributions in the HST brake under external pressure (Model 4)

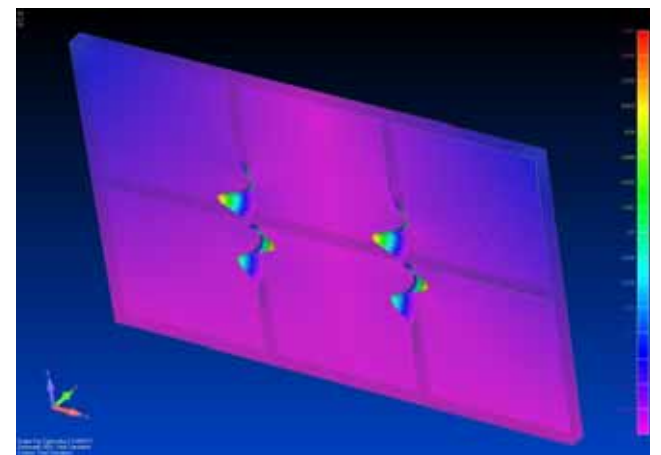


Figure 12. Buckling load of the brake under external pressure (Model 4)

Fig.3.8 illustrates the first buckling mode of the HST brake. The train brake is not critical with respect to buckling behaviour ($l_{\min} = 6.06$).

Conclusions

The subject of this work is the stress and strength analysis of aerodynamic brakes in high-speed trains. Aerodynamic brakes of HSTs are designed as stiffened aluminium plates subjected to lateral pressure loads. The complete computation methodology for the strength/stress analysis of aerodynamic brakes is presented. For that purpose the CFD is used to determine aerodynamic load

and the finite element method (FEM) is used for the stress and stability analysis. In order to obtain the minimum weight of the structure, the initial dimensions of the train brake are reduced in steps to satisfy allowable stresses of aluminium material and buckling load behaviour. The proposed construction design is not critical with respect to buckling loads.

Acknowledgments

This work was financially supported by the Ministry of Science and Technological Development of Serbia under Project TR-35045.

References

- [1] BLAZEK, J.: *Computational Fluid Dynamics – Principles and Applications*, Elsevier, 2001.
- [2] PUHARIĆ, M., LUČANIN, V., RISTIĆ, S., LINIĆ, S.: *Application of the Aerodynamical Brakes on Trains*, Research and Design in Commerce & Industry, ISSN 1451-4117, UDC 33, 8(2010)1, 2010, 168, pp.13-21.
- [3] MAKSIMOVIĆ, S., VASOVIĆ, I., MAKSIMOVIĆ, M., MILUTINOVIĆ, Z., RISTIĆ, M.: *Numerical predictions and experimental verification in fatigue crack growth of aluminum alloy attachment lugs*; ECAA, the Conference on Aluminium Science and Technology 5–7 October 2011, Bremen, Germany.
- [4] KOZIĆ, M., RISTIĆ, S., PUHARIĆ, M., KATAVIĆ, B., PRVULOVIĆ, M.: *Comparison of numerical and experimental results for multiphase flow in duct system of thermal power plant*, Scientific Technical Review, ISSN 1820-0206, 2010, Vol.60, No. 3-4, pp.39-47.
- [5] CLARKE, J.D., NARAYANAN, R.: *Buckling of aluminium alloy stiffened plate ship structure: In: Aluminium structures—advances design and construction*, Proceedings of the international conference on steel and aluminium structures, Cardiff, July 1987, Elsevier, 1987, pp.81–92.
- [6] AALBERG, A., LANGSETH, M., LARSEN, P.K.: *Stiffened aluminium panels subjected to axial compression*. Thin Wall Struct 2001; 39: pp.861–865.
- [7] AALBERG, A., LANGSETH, M., MALO, K.A.: *Ultimate strength of stiffened aluminium plates*. Department of Structural Engineering, Norwegian University of Science and Technology, 1998.
- [8] KHEDMATI, M.R., ZAREEI, M.R., RIGO, P.: *Sensitivity analysis on the elastic buckling and ultimate strength of continuous stiffened aluminium plates under combined in-plane compression and lateral pressure*, Thin-Walled Structures, 2009. doi:10.1016/j.tws.2009.04.010.
- [9] Msc/NASTRAN, *Theoretical Manuals*
- [10] FLUENT, *Theoretical Manuals*
- [11] PUHARIĆ, M., RISTIĆ, S., Kutin, M.: *Istraživanje aerodinamičkog otpora brzih vozova*, Međunarodni naučno-stručni skup Energetska Efikasnost 2008., Vrnjačka Banja, novembar 2008.

Received: 05.05.2011.

Strukturalna analiza aerodinamičke kočnice kod brzog voza

Aerodinamički problem kod vozova su vezani za obstrujavanja oko voza. Pažnja u radu je usmerena na analizu naponskih stanja i gubitak stabilnosti kod konstrukcije vazdušne kočnice brzog voza. Ponašanje aerodinamičke kočnice je analizirano kao orebrena ploča sa uzdušnicima i rebrima pod dejstvom spoljnog pritiska. Za modeliranje ove konstrukcije su korišćeni konačni elementi ljuski. Za analizu naponskih stanja i gubitka stabilnosti korišćen je softverski paket MSC/NASTRAN dok je za određivanje aerodinamičkog opterećenja korišćena CFD analiza koristeći softverski paket FLUENT.

Ključne reči: voz, aerodinamička kočnica, aerodinamičko opterećenje, naponsko stanje, analiza napona, analiza stabilnosti, dinamika fluida, numerička simulacija, metoda konačnih elemenata.

Структурный анализ аэродинамического тормоза у скоростного поезда

Аэродинамические проблемы у железнодорожных поездов тесно связаны с потоками, происходящими вокруг поезда. Основная цель и внимание этой работы направлены на анализ состояния напряжённых состояний и потери устойчивости в конструкции аэродинамического тормоза высокоскоростных поездов (HST). Поведение аэродинамического тормоза определяется как застывшая пластина с рёбрами, подвергающаяся боковым нагрузкам и влиянию внешнего давления. Для моделирования этой структуры были использованы конечные элементы снарядов. Для анализа напряжённых состояний и потери устойчивости использован программный пакет MSC / NASTRAN, пока для определения аэродинамических нагрузок использован CFD анализ с употреблением программного пакета FLUENT.

Ключевые слова: железнодорожный поезд, аэродинамический тормоз, аэродинамическая нагрузка, напряжённое состояние, анализ напряжений, анализ устойчивости, динамика жидкостей, численное моделирование, метод конечных элементов.

Analyse structurale du frein aérodynamique chez le train rapide

Les problèmes aérodynamiques chez les trains sont étroitement liés aux courants autour du train. Dans ce travail l'attention principale est prêté à l'analyse des états de tension et à la perte de la stabilité chez la construction du frein aérien du train rapide. Le comportement du frein aérodynamique a été analysé comme une plaque à nervures sous l'action de la pression extérieure. Pour la modélisation de cette construction on a utilisé les éléments finis des coques. Le progiciel MSC/NASTRAN a été employé pour l'analyse des états de tension et de la perte de stabilité tandis que l'analyse CFD a été appliquée pour la détermination de la charge aérodynamique .

Mots clés: frein aérodynamique, charge aérodynamique, état de tension, analyse de tension, analyse de stabilité, dynamique des fluides, simulation numérique, méthode des éléments finis